

## Efficient Wing Design for Complex Aircraft Configuration Using CAD, Unstructured CFD and Inverse Problems

Takeshi FUJITA,

Department of Aeronautics and Space Engineering, Tohoku University

01 Aramaki-Aza-Aoba, Aoba-ku, Sendai, 980-8579, JAPAN

*Keywords: SST, Inverse Wing Design, Aerodynamics, CFD*

### Abstract

*An efficient aerodynamic design system is developed and applied to designing natural laminar flow wings of the experimental supersonic airplanes of National Aerospace Laboratory (NAL) in Japan. In the developed design system, the design phase employs an inverse problem solver using integral equations. The analysis phase uses an unstructured-grid CFD so as to treat full configurations of airplanes efficiently. Interfaces among the design phase, analysis phase and CAD are also developed. The newly developed method has advantages of the efficiency and wide applicability to complicated configurations of airplanes. Its capability is demonstrated for the wing design coupled with the full configuration flow analysis.*

### 1 Introduction

Currently a next generation Supersonic Transport (SST) is under research at the National Aerospace Laboratory in Japan (NAL) [1], collaborating with industries and universities, one of which is the Tohoku University. Those models are scaled into 1/10 of the real commercial passenger airplanes. In the first stage of this project called NEXST-1 (see Fig. 1), an un-powered supersonic experimental airplane

was developed. It will be launched for the flight tests at Woomera prohibited area in Australia in 2002. In the second stage called NEXST-2, an experimental airplane equipped with existing jet propulsion system YJ-69 is under development and the aerodynamic design of 1<sup>st</sup> configuration was finished as a prototype model (see Fig. 2). The NEXST-2 will be flight tested in 2005.

The NAL project aims to reduce the drag with the concept for the wing design of Natural Laminar Flow (NFL) on the upper surface and elliptical load distribution along the spanwise direction. It also aims to establish a CFD-oriented design system. With the design goal of the NLF concept, it is needed to design airfoil geometry precisely at each span-station so as to realize the special form of pressure distribution on the wing surface at the cruising condition [2]. For this purpose, a new design method, which can determine the airfoil geometry at each span-station using specified pressure distribution as a boundary condition, has been formulated and developed [3][4][5].

The NEXST-1 does not have the propulsion system so that the configuration is relatively simple as shown in Fig. 1. Therefore, the wing design had been conducted by a combination of the inverse problem solver and the conventional structured-grid CFD. In contrast, the NEXST-2 model has a fairly large propulsion system.

Therefore an interaction between the wing and the propulsion system must be taken into account (see Fig. 3). The geometrical complexity makes it difficult to use the conventional structured-grid CFD because of the painfully slow turnaround time. It should be needed to efficiently evaluate aerodynamic performance for this complex configuration and to effectively combine this evaluation with the inverse problem solver.

In general, most of design algorithms need several hundred times of flow simulation during the design process. For the inverse design system, in contrast, it is known from the experience that the number of flow simulations required is less than twenty, which is a very small number as compared with other design methods. Even with this small number, it took several days to perform one flow simulation by a conventional CFD system because of time-consuming process of the grid generation for complex configuration. Besides the mesh generation, inconsistent usage of boundary conditions for the inverse solver and the CFD simulation needs other time-consuming works for designers.

To overcome the cause, unstructured-grid CFD was utilized in this study. We have already systematized pre-process of unstructured grid (see Fig. 4). The computational time of the flow solver for the Euler equations was drastically reduced by the LU-SGS implicit method and the parallelization using the MPI library. With this CFD system, it takes only one day per simulation to evaluate aerodynamics.

In this paper, a short turn-around inverse design system that can execute one cycle of inverse under one day developed in this study is described, where the inverse is effectively coupled with the unstructured-grid CFD system as shown in Fig. 5. The capability of the system is demonstrated by applying it to the wing design

of the NEXST-2 model.

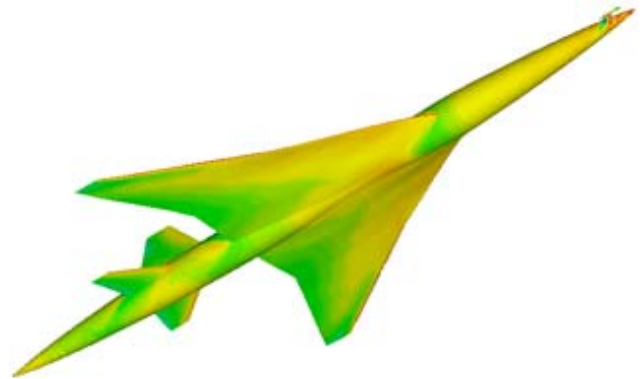


Fig. 1 Pressure Distribution of NEXST-1  
at  $M_\infty = 2.0$ ,  $\alpha = 0.0\text{deg}$ .

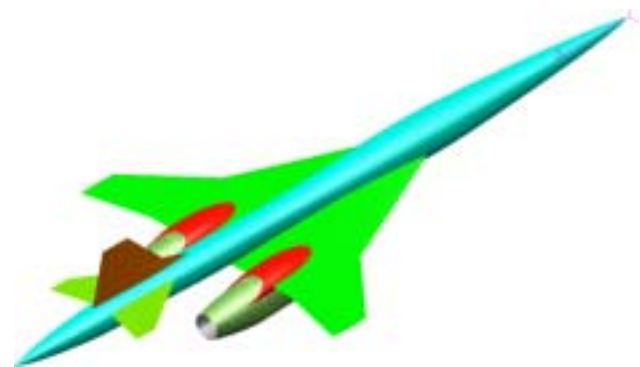


Fig. 2 NAL NEXST-2

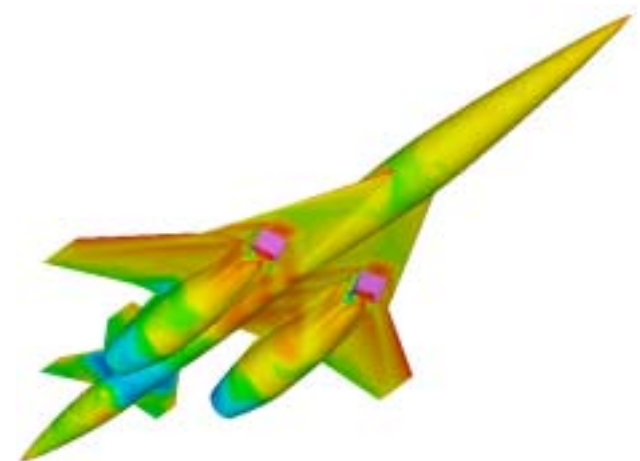


Fig. 3 Pressure Distribution of NEXST-2  
at  $M_\infty = 1.7$ ,  $\alpha = 0.0\text{deg}$ .

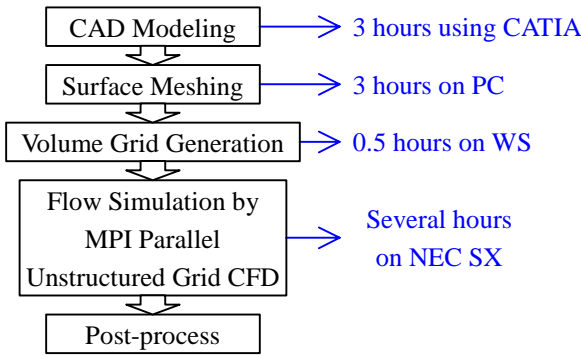


Fig. 4 CFD Process

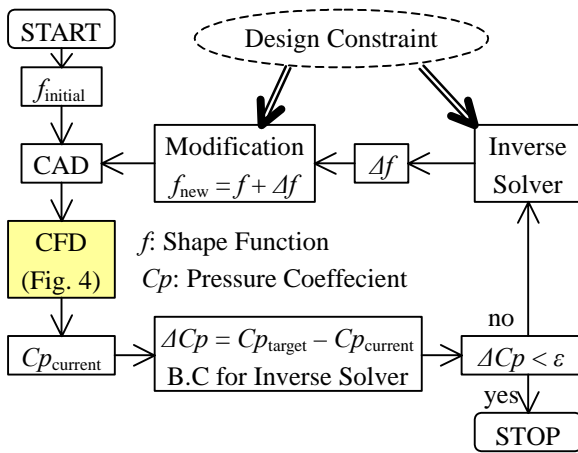


Fig. 5 Design Procedure

## 2 Inverse Design and the Interface with CAD or CFD

### 2.1 Inverse design method

The present design procedure for wings is iterative method. Figure 5 illustrates the procedure. The method determines the wing section's geometry, which realizes a specified target pressure distribution at all span stations of a wing. First, a baseline shape is to be guessed. Then the flow field around the wing is analyzed by flow simulation to get the current pressure coefficient ( $C_p$ ) distribution on the wing surface. Next the inverse problem is solved to obtain the geometrical correction value ( $\Delta f$ ) corresponding to the difference between target and current pressure distributions ( $\Delta C_p$ ). The new wing is defined by modifying the baseline shape using  $\Delta f$ .

Now, the current shape is updated. The next step is to go back to the flowfield analysis. The flow analysis is conducted to see whether the current shape realizes target pressure distribution or not. If the difference between target and current pressure distributions is negligible, the design is completed. Otherwise, the next step is once again to solve the inverse problem and iterate the design loop until the pressure difference becomes negligible. This iterative procedure of reducing the residual is widely used in numerical aerodynamic design.

### 2.2 Interface between flow simulation and inverse design

Since the wing near the symmetry plane is overlapped by the fuselage, the airfoil covered in the fuselage is exterminated by linearly extrapolating the 15% semi-span airfoil, as shown in Fig. 6. For the extrapolation, quadratic extrapolation of the leading/trailing edge is performed inside 3% semi-span to connect the leading edge curve smoothly to the opposite side of a half wingspan at a symmetry plane. It implies the removal of the apex singularity.

### 2.3 Interface between inverse design and CAD

The inverse problem solver in this study is formulated from supersonic small perturbation theory [5]. So perturbation of the freestream direction, which is chordwise, is mostly considered, but the spanwise direction is not carefully considered. The solver takes care of the smoothness in chordwise direction. It overlooks that in spanwise direction. Therefore the inverse problem result sometimes oscillates in the spanwise direction. This caused harmful effect on the following process of the design loop, so we smoothens the designed geometry using the least squares approximation by a 5<sup>th</sup> degree

polynomial function, as shown in Fig. 7.

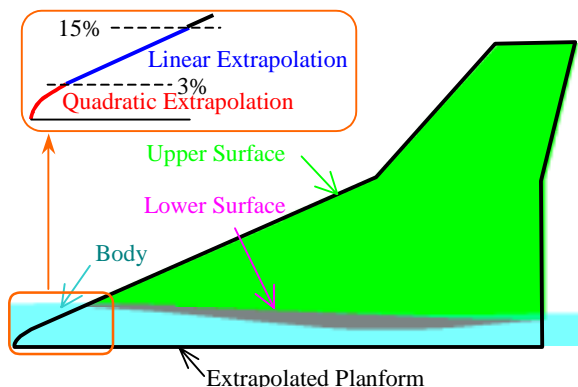


Fig. 6 Extrapolated Wing Planform

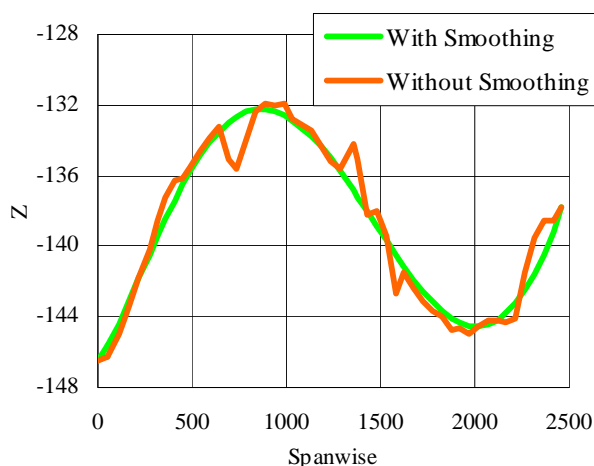


Fig. 7 Comparison of Trailing Edge Line in Spanwise Direction with/without Smoothing

### 3 CFD Evaluation System

CFD pre-process of unstructured grid have been already systematized (see Fig. 4). A configuration is defined using the CATIA, which is commercial CAD software. And several modification techniques, devised by the author, are applied and surface geometry data are obtained by Stereolithography (STL) file [6]. Then the Edge Editor, a surface meshing software developed at the Tohoku University [7], is used to generate the surface grid with advancing front method. Finally the volume grid is automatically generated using Delaunay tetrahedral meshing [8].

The Euler equations are solved by a solution algorithm based on a finite volume cell-vertex scheme for arbitrary shaped cells [9]. The control volume is no overlapping dual cells constructed around each node. To enhance the accuracy, a linear reconstruction of the primitive variables inside the control volume is applied with Venkatakrishnan's limiter [10]. The flux is computed using a HLLW approximate Riemann solver [11]. The computational efficiency is improved by the lower-upper symmetric Gauss-Seidel implicit method with a reordering algorithm for unstructured grids [9]. This implicit time integration method does not require extra storage, and its performance is similar to that of structured grid schemes.

Further reduction of the computational time is introduced by parallelizing the unstructured-grid CFD solver using Message Passing Interface (MPI) library [12][13]. First, an unstructured volume grid is divided by the mesh partitioner based on the METIS, which is developed at the University of Minnesota [14]. Then the partitioned sub-domains are distributed to each processor of a cluster of machines for the parallel execution. The neighboring sub-domains are overlapped by one mesh point. The physical quantity, control volume gradient and limiter at overlapping mesh are sent from "sending vertex" to corresponding "receiving vertices" in other sub-domains. The  $C_p$  distribution for ONERA M6 at 65% semi-span section using parallel solver is compared to the original Euler solver and the experiment in Fig. 8. This figure indicates that the verification of this parallel solver is a good enough. Speedup result for a large size Navier-Stokes (NS) computation on NEC SX-4 vector machine of the Super-Computing System Information Synergy Center in the Tohoku University is shown in Fig.

9. The hybrid grid contains 2,180,582 nodes, 3,839,284 tetrahedrons and 2,943,184 prisms, and this NS computation requires 4 GB memories. This parallel solver achieves extremely good scalability.

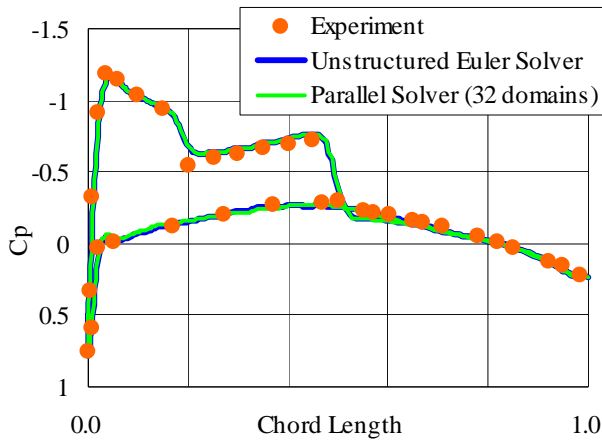


Fig. 8 Comparison of Computed  $C_p$  Distribution with experiment for ONERA M6 at 65% Semi-span Section

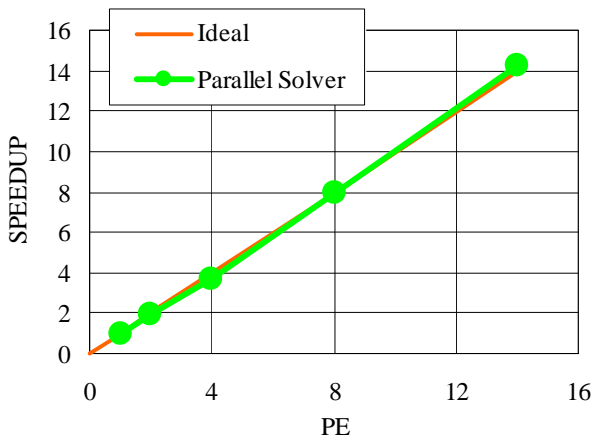


Fig. 9 Speedup for Large Size NS Computation (4 GB) on NEC SX-4 Vector Machine

#### 4 Inverse Design for NAL NEXST-2 Wing

Main wing of the NAL NEXST-2 is designed using the inverse design system. The inner part of the wing is designed to be a NLF wing, and outer part is designed to have a supersonic leading edge. This NLF concept is embodied by a target  $C_p$  distribution. Inverse

design is performed for the wing shape to achieve the target  $C_p$ . Since this is a real design, much constraint has to be satisfied. The wing thickness is constrained by the lowest limit, because the airplane has a large propulsion system in comparison with the body. Sometimes thickness constraint is not consistent with the target pressure distribution. For this NEXST-2 design, the thickness constraint was given first priority over the achievement of the target  $C_p$  at the rear part of wing, which was after 65% chord length. And the nacelle protrudes on the upper surface at the rear part of the wing as shown in Fig. 10. This is a part of reason that we have to give up achieving the target  $C_p$  after 65% chord.

Because of the practical reason of time limit for the project, we take a simple strategy. Thus, we assumed that the interaction effect between a wing and a nacelle is linear. This was justified by Fig. 11, which shows the comparison of  $C_L$ 's with/without nacelle. This figure indicates the effect of the nacelle interaction on  $C_L$  is constant as much as 0.04. So, the preliminary first stage design has been done without considering the nonlinear effect of the nacelle.

The convergence history of the process of NEXST-2 wing inverse design is shown in Fig. 12. The residual is defined as

$$Residual = \frac{\sqrt{\sum (C_p^T - C_p^C)^2}}{N}$$

where  $C_p^T$  and  $C_p^C$  indicate target and current pressure coefficient distributions,  $N$  is the number of nodes on the wing surface. It can be seen that most of the changes to the geometry took place within the first 2 iterations. But the  $C_p$  didn't reach the expansion level of the target  $C_p$  in the vicinity of the leading edge as shown in Fig. 13. We concluded that the first target  $C_p$  was not realistic. So new target  $C_p$  was redefined

by translating the original one slightly into higher level of pressure. It was confirmed that the new target  $C_p$  realized the NLF. These two targets are shown in Fig. 13. This change made the deviation between target and realized current  $C_p$  smaller than the first one.

The initial, final and target  $C_p$  distributions and the corresponding airfoil shapes are shown in Fig. 14 and Fig. 15. The  $C_p$  of the upper surface before 50% chord length at 20% semi-span section agrees well with the target  $C_p$ . But the deviation between target and current  $C_p$  at 40% semi-span section is not small. It was difficult to realize the target  $C_p$  at 40% semi-span section, because of the thickness constraint. The initial and final pressure distributions are shown in Fig. 16 and Fig. 17. A region where pressure shows step function type distribution becomes wider at the upper surface of the final model. Fortunately, the 7<sup>th</sup> inverse designed model was adopted as the NEXST-2 main wing.

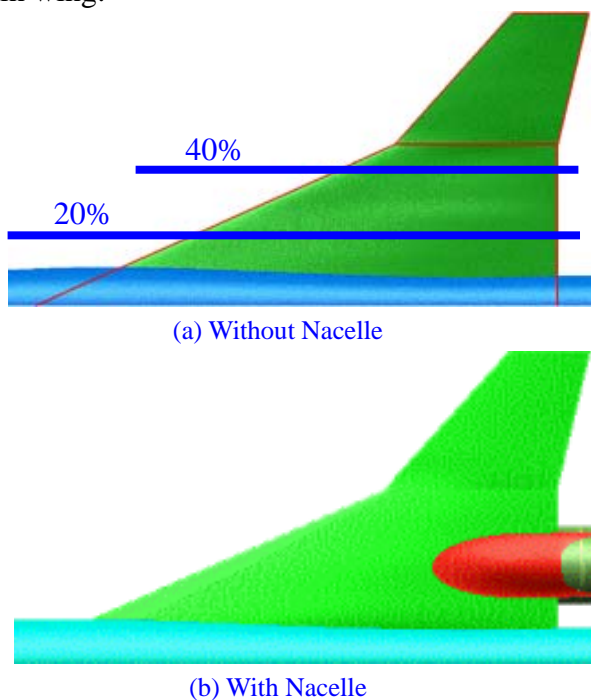


Fig. 10 Upper Surface geometry of Main Wing with/without Nacelle

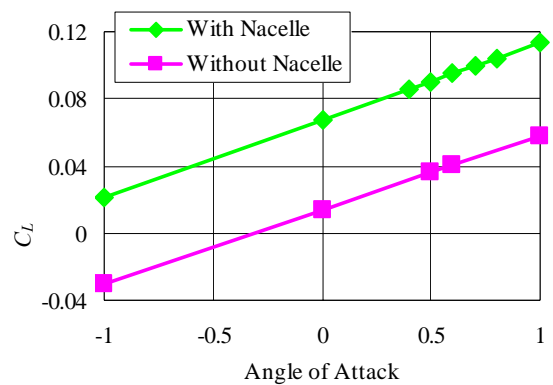


Fig. 11 Comparison of  $C_L$ 's with/without Nacelle

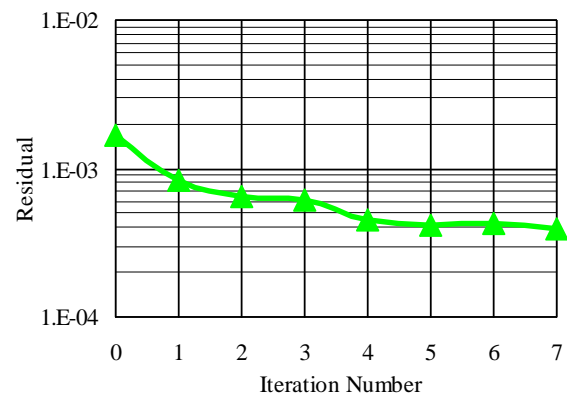


Fig. 12 Convergence History

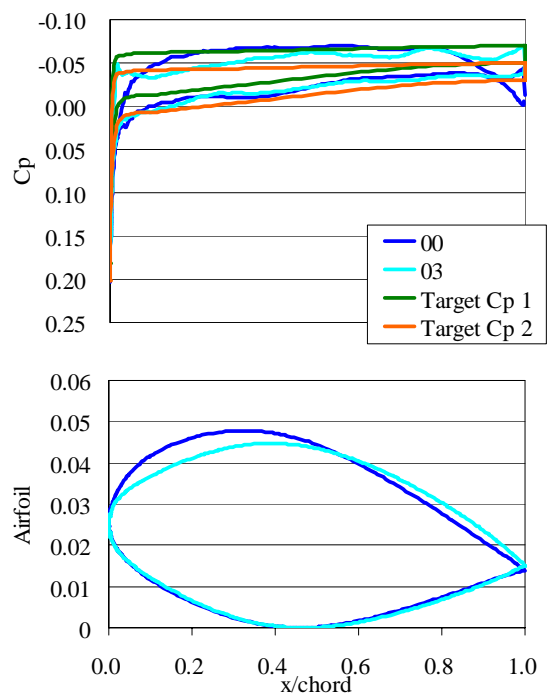


Fig. 13 Comparison of Two Targets, Initial and Inverse Designed Airfoil 3<sup>rd</sup> at 20% Semi-Span

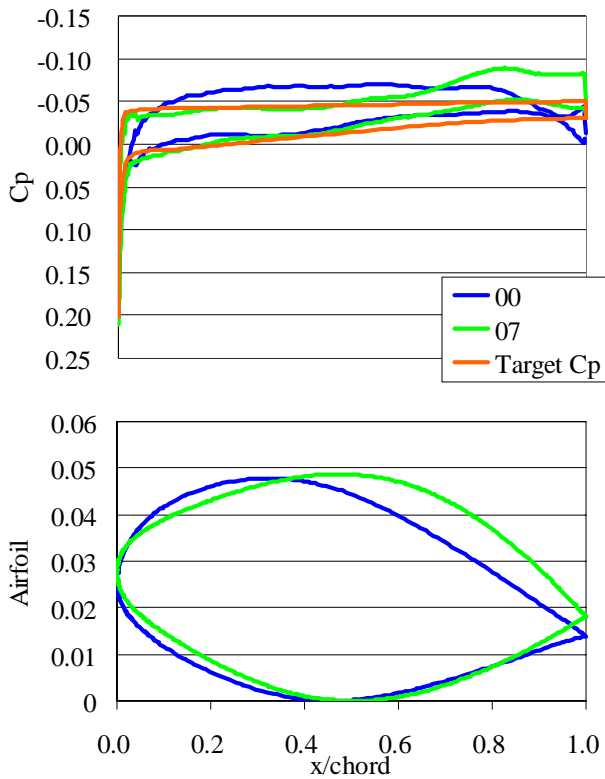


Fig. 14 Initial, final and target  $C_p$  distributions and corresponding airfoil profiles at 20% Semi-Span

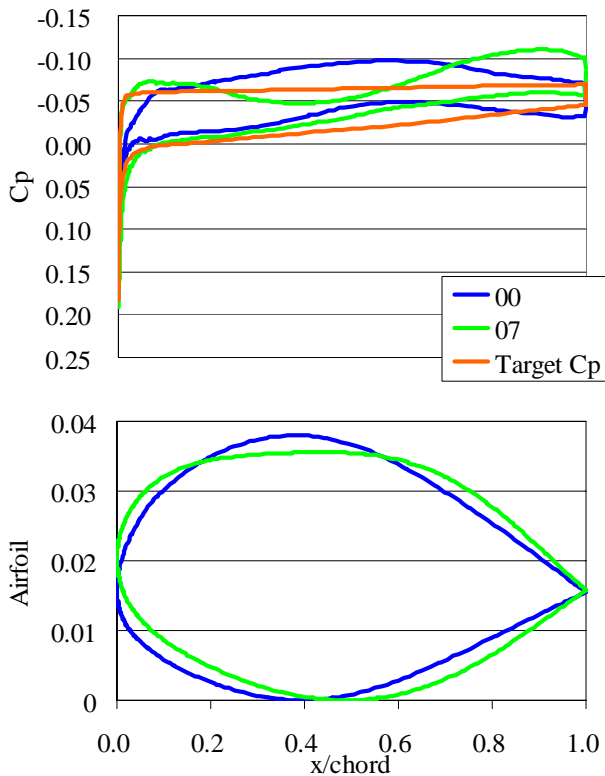


Fig. 15 Initial, final and target  $C_p$  distributions and corresponding airfoil profiles at 40% Semi-Span

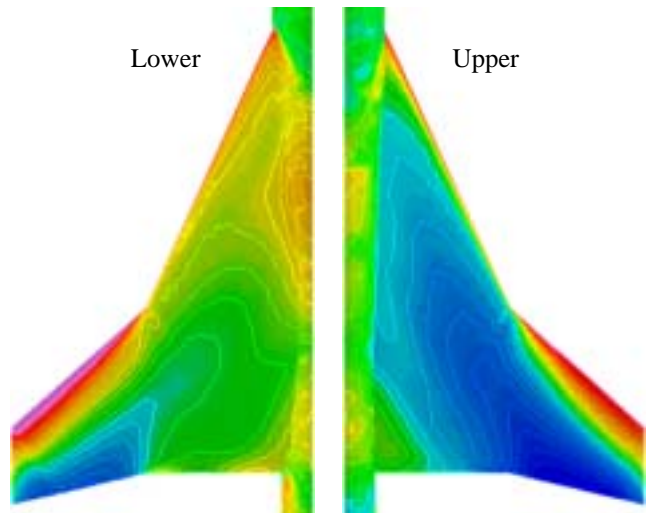


Fig. 16 Pressure Distribution of Initial Configuration

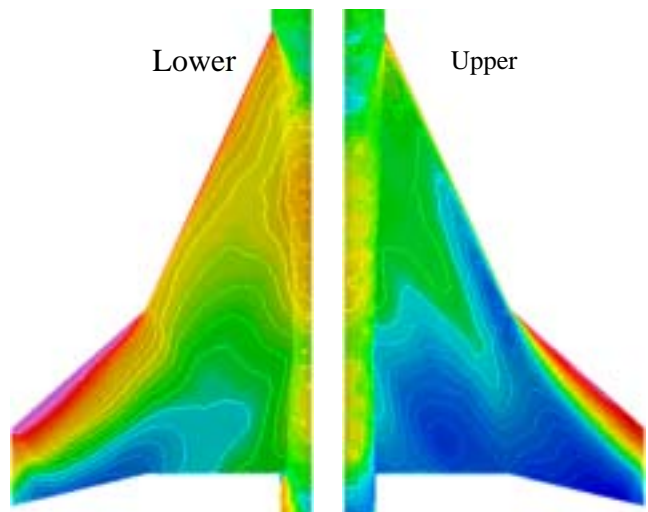


Fig. 17 Pressure Distribution of Designed Configuration

## 5 Conclusions

With the aim of a highly practical and efficient aerodynamic design by CFD, an inverse design method coupled with unstructured-grid CFD was developed. It was applied to aerodynamic design of wings for the NAL experimental supersonic airplane. The design phase was performed by an inverse problem solver using integral equations. The analysis phase of the system employed unstructured-grid CFD closely coupled with CAD system. Furthermore, interfaces among the design,

analysis and CAD were constructed so as to smoothly transfer the appropriate interface data. The newly developed method is efficient and has a wide applicability to complicated configurations of airplanes. With this method, the wing design of the NEXST-2 model was finished within a month, which was much shorter period than the method used before.

### Acknowledgement

The author would like to thank the aerodynamic group of the NEXST project of the NAL JAPAN for their providing the opportunity to join the project. I also would like to thank them for their permission to present geometry data of their SST model in this article. The calculations were performed using the SGI Origin 2000 and the NEC SX-5 in the Institute of Fluid Science, Tohoku University and the NEC SX-4 in the Super-Computing System Information Synergy Center, Tohoku University. Also, special thanks go to Mr. Y. Ito of the Tohoku University for his help and support about grid generation. Finally, the author would like to thank the New Energy and Industrial Technology Development Organization (NEDO) of Japan. The present study was supported by the Industrial Technology Research Grant Program in '01A53001d from NEDO of Japan.

### References

- [1] Sakata K. Supersonic Experimental Airplane Program in NAL and Its CFD-Design Research Demand. *NAL's 2<sup>nd</sup> SST-CFD Workshop*, pp.53-56, 2000.
- [2] Shimbo Y, Yoshida K, Iwamiya T, R Takaki and Matsushima K. Aerodynamic Design of Scaled Supersonic Experimental Airplane. *NAL's 1<sup>st</sup> SST-CFD Workshop*, pp. 62-67, 1998.
- [3] Jeong S, Matsushima K, Iwamiya T, Obayashi S and Nakahashi K. Inverse Design Method for Wings of Supersonic Transport. *36<sup>th</sup> Aerospace Science Meeting & Exhibit*, Reno (NV, USA), AIAA paper 98-0602, 1998.
- [4] Matsushima K, Iwamiya T, Jeong S and Obayashi S. Aerodynamic Shape Design of a Wing for NAL's SST using an Inverse Problem. *Proceedings of Aerospace Numerical Simulation Symposium '98*, Tokyo (Japan), pp.191-pp.196, 1999.
- [5] Matsushima K. Improper Integrals in the Formulation of a Supersonic Inverse Problem. *Inverse Problems in Engineering Mechanics II*, Elsevier Science Ltd., pp. 399-405, 2000.
- [6] Fujita T, Ito Y, Nakahashi K and Iwamiya T. Computational Fluid Dynamics Evaluation of National Aerospace Laboratory Experimental Supersonic Airplane in Ascent. *Journal of Aircraft*, Vol. 39, No. 2, pp. 359-364, 2002.
- [7] Ito Y and Nakahashi K. Direct Surface Triangulation Using Stereolithography Data. *AIAA Journal*, Vol. 40, No. 3, pp. 490-496, 2002.
- [8] Sharov D and Nakahashi K. A Boundary Recovery Algorithm for Delaunay Tetrahedral Meshing. *Proceedings of the 5<sup>th</sup> International Conference on Numerical Grid Generation in Computational Field Simulations*, International Society of Grid Generation, pp. 229-238, 1996.
- [9] Sharov D and Nakahashi K. Reordering of Hybrid Unstructured Grids for Lower-Upper Symmetric Gause-Seidel Computations. *AIAA Journal*, Vol. 36, No. 3, pp. 484-486, 1998.
- [10] Venkatakrishnan V. On the Accuracy of Limiters and Convergence to Steady-State Solutions. *31<sup>st</sup> Aerospace Sciences Meeting & Exhibit*, Reno (NV, USA), AIAA paper 93-0880, 1993.
- [11] Obayashi S and Guruswamy G P. Convergence Acceleration of a Navier-Stokes Solver for Efficient Static Aeroelastic Computations. *AIAA Journal*, Vol. 33, No. 6, pp. 1134-1141, 1995.



- [12] D. J. Mavriplis. Parallel Unstructured Mesh Analysis of High-lift Configurations. *38<sup>th</sup> Aerospace Sciences Meeting & Exhibit*, Reno (NV, USA), AIAA Paper 2000-0923, 2000.
- [13] Fujita T, Koizumi T, Kodera M, Nakahashi K, Iwamiya T, Nakamura T. Evaluation of Parallelized Unstructured-Grid CFD for Aircraft Applications. *Proceedings of Parallel CFD 2002*, Kyoto (Japan), pp.103-pp.106, 2002.
- [14] <http://www-users.cs.umn.edu/~karypis/>